S2.EXTREME 2014 FIRE SEASON IN CALIFORNIA: A GLIMPSE INTO FUTURE?

Jin-Ho Yoon, S.-Y. Simon Wang, Robert R. Gillies, Lawrence Hipps, Ben Kravitz, and Philip J. Rasch

This document is a supplement to "Extreme 2014 Fire Season in California: A Glimpse into Future?," by Jin-Ho Yoon, S.-Y. Simon Wang, Robert R. Gillies, Lawrence Hipps, Ben Kravitz, and Philip J. Rasch (*Bull. Amer. Meteor. Soc.*, **96** (12), S5–S9) • DOI:10.1175/BAMS-D-15-00114.1

Model output: Thirty ensemble members were produced by the Community Earth System Model version 1 (CESM1) with spatial resolution of 0.9° longitude × 1.25° latitude through the Large Ensemble Project (Kay et al. 2014). The simulations cover two periods: (1) 1920–2005 with historical forcing, including greenhouse gases, aerosol, ozone, land use change, solar and volcanic activity, and (2) 2006–80 with RCP8.5 forcing (Taylor et al. 2012). The ensemble spread of initial conditions is generated by the commonly used "round-off differences" method (Kay et al. 2014). The CESM1 was used here partly because it performs well on the depiction of the ENSO cycle and ENSO precursors and associated teleconnection towards North America (Wang et al. 2013, 2014).

Burned Area from the GFED4: This product combines burned area mapped at 500-m resolution from Moderate-Resolution Imaging Spectroradiometer (MODIS) mission with active fire data from both Tropical Rainfall Measuring Mission (TRMM) Visible and Infrared Scanner (VIRS) and the Along-Track Scanning Radiometer (ATSR) sensors with the spatial resolution of 0.25° for the period of June 1996–December 2014 (Giglio et al. 2013).

Keetch–Byram Drought Index (KBDI): The KBDI (Keetch and Byram 1968) has been routinely used for the monitoring of fire danger over the contiguous United States by the U.S. Forest Service (e.g., www.wfas.net/images/firedanger/kbdi.png). Daily mean precipitation and daily maximum temperature are required. Both observational and simulated datasets are used to compute the KBDI. Observational dataset is obtained from the North American Land Data Assimilation system phase 2 (NLDAS2; Xia et al. 2012) for the period of 1979–current at 1/8° resolution. In this study, a computational formula by Janis et al. (2002) is adopted.

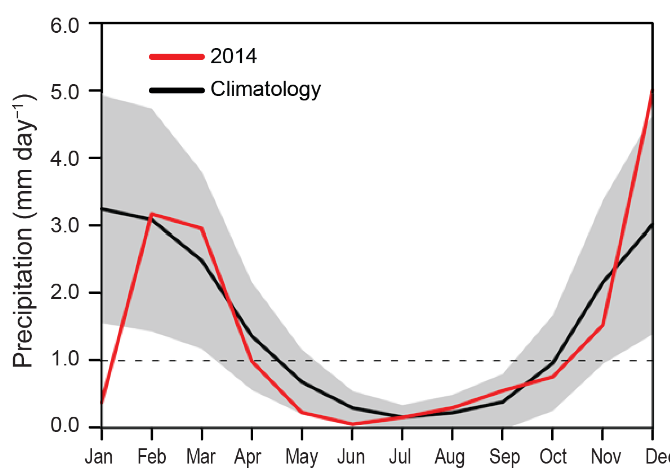

Fig. S2.1. Monthly precipitation (mm day^{-1}) averaged over California using CPC Unified precipitation dataset (Chen et al. 2008; Xie et al. 2007). Red line indicates precipitation in year 2014. Black is for the long-term climatology with one standard deviation at each month.

Extreme fire risk measure by (i) fractional area under extreme fire risk and (ii) extreme fire danger days: To display how frequent or large area is under the threat of the extreme fire risk, fractional area under extreme fire risk is computed. Extreme fire risk is defined as the KBDI larger than 600. On each day, area with the KBDI value larger than 600 is identified and its fraction compared to the larger domain is computed for either the entire or northern part of California (Figs. S2.1 and S2.2 show its annual mean). We also count the number of days per year with the area-averaged KBDI values over northern (north of 39°N), central (36°–39°N), and southern (south of 36°N) California (Fig. S2.2c).

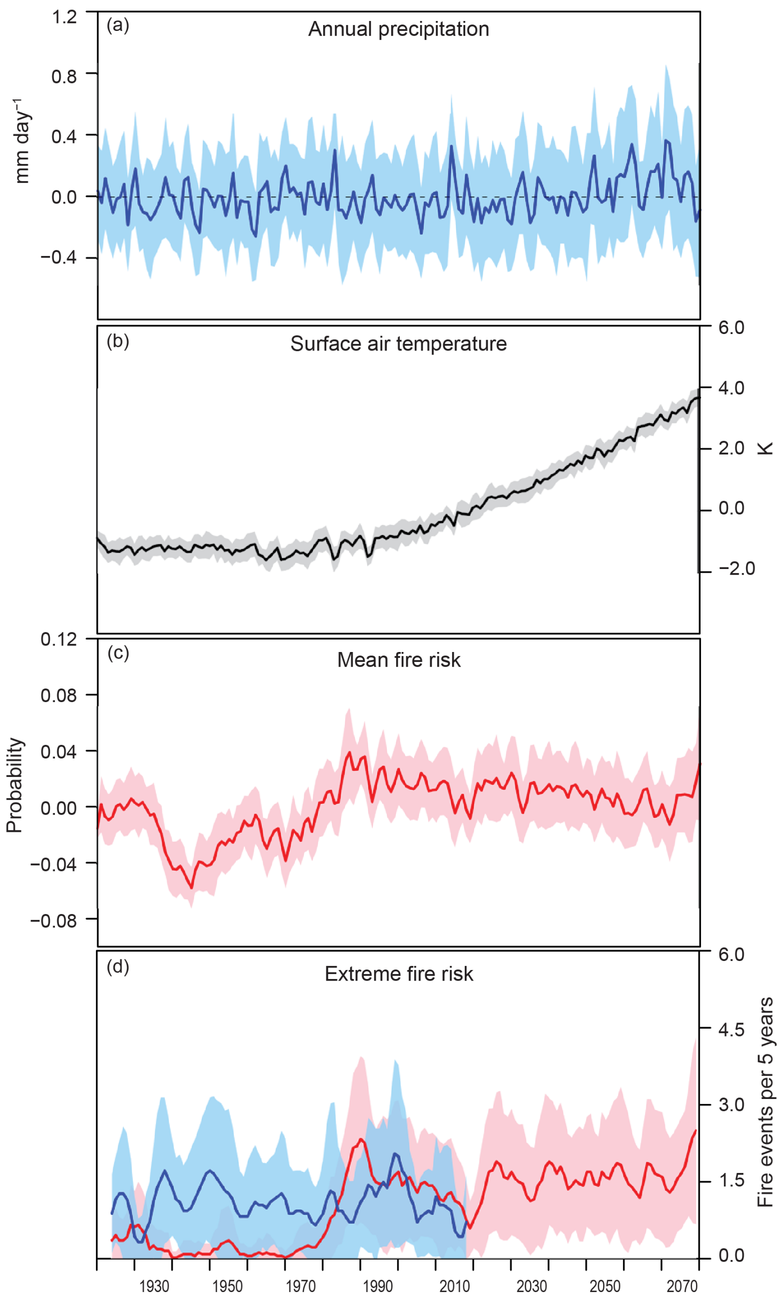

Fig. S2.2. (a) Annual mean precipitation anomaly (mm day⁻¹), (b) surface air temperature anomaly (°C), (c) mean fire risk, and (d) occurrences of extreme fire event over California counted within a moving 5-year window. Historical (1920–2005) and future based on RCP8.5 scenario (2006–80) are colored red and preindustrial simulation is in blue.

Ensemble spread: Throughout this work, a shaded area indicates the middle 50% of the spread of the ensemble members, calculated using z * standard deviation. In a normal distribution, the z value for 50% is 0.674490.

Rainfall seasonal cycle in 2014: Seasonal cycle of rainfall averaged over California is shown in Fig. S2.1. California rainfall exhibits clear seasonal cycle with dry season roughly in May–September. In 2014, rainfall in April is around 1 mm day^{-1} and that in May is almost zero. Thus, by treating monthly rainfall less than 1 mm day^{-1} as an indicator of the dry season, 2014 started two weeks early.

Simulated fire probability: A prognostic fire algorithm was coupled with the sophisticated land modules in the CESM1 to generate fire parameters such as fire probability and burned area fraction, based upon fuel availability and near-surface soil moisture condition (Thonicke et al. 2001). This capability allows us to assess directly the effect of greenhouse gases on climate oscillations, precipitation anomalies, and their impact on wildfires. Annual mean fire probability averaged over California shows permanent increase after 1970 (Fig. S2.2c), but the increase ceases at the end of the 20th century and restarts at the end of the 21st century. Here the "extreme fire risk" for California is defined as the occurrence of extreme annual-mean fire probability (exceeding

1.5 standard deviation) in Fig. S2.2d during any given 5-year period. Figure S2.2d shows that the CESM1 extreme fire risk in California increases slightly in the historical period, though its pace of increment becomes much faster toward the latter part of the 21st century indicating more and/or increased wildfire.

Total precipitation and surface temperature changes: Precipitation and surface air temperature averaged over California (Figs. S2.2a,b).

REFERENCES

Chen, M., W. Shi, P. Xie, V. B. S. Silva, V. E. Kousky, R. W. Higgins, and J. E. Janowiak, 2008: Assessing objective techniques for gauge-based analyses of global daily precipitation. *J. Geophys. Res.*, **113**, D04110, doi:10.1029/2007JD009132.

Giglio, L., J. T. Randerson, and G. R. van der Werf, 2013: Analysis of daily, monthly, and annual burned area using the fourth-generation global fire emissions database (GFED4). *J. Geophys. Res. Biogeosci.*, **118**, 317–328, doi:10.1002/jgrg.20042.

Janis, M. J., M. B. Johnson, and G. Forthun, 2002: Near-real time mapping of Keetch-Byram drought index in the south-eastern United States. *Int. J. Wildland Fire*, **11**, 281–289.

Kay, J. E., and Coauthors, 2015: The Community Earth System Model (CESM) Large Ensemble Project: A community resource for studying climate change in the presence of internal climate variability. *Bull. Amer. Meteor. Soc.*, **96**, 1333–1349, doi:10.1175/BAMS-D-13-00255.1.

Keetch, J. J., and G. M. Byram, 1968: A drought index for forest fire control. U.S.D.A. Forest Service Res. Paper SE-38, 32 pp. [Available online at www.srs.fs.usda.gov/pubs/rp/rp_se038.pdf.]

Taylor, K. E., R. J. Stouffer, and G. A. Meehl, 2012: An overview of CMIP 5 and the experiment design. *Bull. Amer. Meteor. Soc.*, **93**, 485–498, doi:10.1175/BAMS-D-11-00094.1.

Thonicke, K., S. Venevsky, S. Sitch, and W. Cramer, 2001: The role of fire disturbance for global vegetation dynamics: Coupling fire into a Dynamic Global Vegetation Model. *Global Ecol. Biogeogr.*, **10**, 661–677.

Wang, S.-Y., M. L'Heureux, and J.-H. Yoon, 2013: Are greenhouse gases changing ENSO precursors in the western North Pacific? *J. Climate*, **26**, 6309–6322, doi:10.1175/JCLI-D-12-00360.1.

——, L. Hipps, R. R. Gillies, and J. H. Yoon, 2014: Probable causes of the abnormal ridge accompanying the 2013-2014 California drought: ENSO precursor and anthropogenic warming footprint. *Geophys. Res. Lett.*, **41**, 3220–3226, doi:10.1002/2014GL059748.

Xia, Y. L., and Coauthors, 2012: Continental-scale water and energy flux analysis and validation for the North American Land Data Assimilation System project phase 2 (NLDAS-2): 1. Intercomparison and application of model products. *J. Geophys. Res.*, **117**, D03109, doi:10.1029/2011JD016048.

Xie, P., A. Yatagai, M. Chen, T. Hayasaka, Y. Fukushima, C. Liu, and S. Yang, 2007: A gauge-based analysis of daily precipitation over East Asia. *J. Hydrometeor.*, **8**, 607–626.